Ionic liquids for electrochemical devices

AUTHOR(S):

HAGIWARA, Rika; LEE, Je Seung

CITATION:

HAGIWARA, Rika ...[et al]. Ionic liquids for electrochemical devices. Electrochemistry 2007, 75(1): 23-34

ISSUE DATE:

2007-01-05

URL:

http://hdl.handle.net/2433/260564

-Review-

Ionic Liquids for Electrochemical Devices

Rika Hagiwara and Je Seung Lee

Graduate School of Energy Science, Kyoto University, Sakyo-ku, Kyoto 606-8501, Japan
hagiwara@energy.kyoto-u.ac.jp

Received September **; Accepted ** **, 2006

A short review of ionic liquids (ILs) and their applications as electrolytes for electrochemical devices, such as electrical double layer capacitors, fuel cells, lithium batteries, and solar cells, are presented here. The properties of ILs, such as non-volatility, non-flammability, wide liquid temperature ranges, and wide electrochemical windows, have the potential to be improved, including improvements in durability and safety, extending the operational temperature ranges and enabling improvements in power and energy densities of the devices.

Key Words: Ionic Liquid, Molten Salt, Capacitor, Fuel Cell, Battery, Solar Cell, Actuator

1 Introduction

Molten salts, such as sodium chloride, are classified as high temperature ionic liquids that require high temperatures to melt. However, some salts, mostly organic, are known to melt at around or below room temperature. These salts with low melting points (typically lower than 100ºC) are called ionic liquids (ILs) currently, although the original definition did not include a temperature limitation. When ILs are used as electrolytes in electrochemical devices, a number of advantages are expected: non-volatility makes their handling easier and prevents the electrolyte from drying; non-flammability improves safety of the devices; a wide electrochemical window

raises power and energy densities; and a wide liquid-phase temperature range enables the operation of the devices in various environments. In 1992, 1-ethyl-3-methylimidazolium tetrafluoroborate ([EMIm]BF_4) and 1-ethyl-3-methylimidazolium triflate ([EMIm]CF_3SO_3), were reported as novel moisture-stable ILs for the first time [1,2]. Subsequently, a wide variety of moisture-stable ILs have been reported and applied as reaction solvents in organic syntheses. Most of the moisture-stable ILs reported thus far contain organic or inorganic fluoroanions as counter anions that are combined with some onium cations [3-7]. Some of the potential applications of ILs as electrolytes such as capacitors, fuel cells, lithium batteries, solar cells, and actuators are described in this review.

2 Synthesis of ionic liquids

2.1 Molecular design of ionic liquids as electrolytes

Figure 1 shows some typical cations used for the synthesis of ILs. They are usually singly charged cations. Atomic or inorganic cations are still not commonly used. As will be described later, the preparation of ILs of lithium salts is challenging from the viewpoint of application to lithium batteries [8]. In general, (1) ILs of aromatic ammonium cations, such as alkylimidazolium and alkylpyridinium ions, exhibit low melting points compared to the ILs of nonaromatic ammonium cations, such as tetraalkylammonium and dialkylpyrrolidinium ions; (2) the chemical and electrochemical stabilities of nonaromatic ammonium cation-based ILs are superior to those of aromatic ammonium cation-based ILs; (3) the melting point and conductivity of an IL decreases with an increase in carbon number of the alkyl side-chain on the cation. In addition, side chains on the cation are also important factors that determine the properties of the salt. Introduction of alkenyl groups sometimes decreases the viscosity and increases the ionic conductivity of ILs [9]. Introduction of perfluoroalkyl groups increases the melting points and limits the anions to be combined [10,11].

In contrast to the variety of cations used, the anions available are still limited, though some atomic and inorganic anions are available in addition to organic anions. Atomic halide anions,

except for fluorides, form ILs with low melting points by combination with some cations. Fluoroanions, wherein some of the fluorine atoms are substituted by perfluoroalkyl groups, $BF_3CF_3^-$ [12,13] and $PF_3(C_2F_5)_3^-$ [14] for example, have been recently developed to produce ionic liquids with high hydrophobicity and/or electrochemical stability.

2.2 Synthetic methods of ionic liquids

For preparation of ILs, halide salts, C^+X^-s ($X = Cl^-$, Br^-, I^-) containing cations for ILs are often used as starting materials. Ammonium halides are prepared by the reaction of halogenoalkane and amine. For example, one of the most popular salts used, 1-butyl-3-methylimidazolium chloride ([BMIm]Cl), is synthesized by the reaction of 1-methylimidazole and chlorobutane in acetonitrile.

$$\text{1-methylimidazole} + CH_3CH_2CH_2CH_2Cl \rightarrow [BMIm]^+Cl^- \quad (1)$$

Except for the reactions of volatile chloroalkanes, such as chloroethane, that are performed in an autoclave, reactions are usually carried out under refluxing. All the reagents need to be well-dried prior to use. The next procedure is the metathesis of C^+X^- and M^+A^- (M^+: alkali metal, silver, or ammonium cation, A^-: anion for IL) in a solvent. One of the preparation methods of $[EMIm]BF_4$ is the reaction of [EMIm]I and $AgBF_4$ in a water/methanol solvent [1].

$$C^+X^- + M^+A^- \rightarrow C^+A^- + M^+X^- \quad (2)$$

Since ILs are non-volatile and cannot be distilled in general, the byproduct M^+X^- is removed only by filtration or extraction. However, the halide is not completely eliminated in this procedure because the solubility of M^+X^- in IL is not absolutely zero. In the case of a water-insoluble salt such as 1-ethyl-3-methylimidazolium bis(trifluoromethanesulfone) amide ($[EMIm](CF_3SO_2)_2N$), washing with water is an effective method to remove halide impurities. A protic acid H^+A^- or its

solution is occasionally used instead of M^+A^-, for which the byproduct H^+X^- is completely removed from the IL obtained *in vacuo* at elevated temperatures.

$$C^+X^- + H^+A^- \rightarrow C^+A^- + H^+X^-\uparrow \quad (3)$$

Fluorohydrogenate salts are synthesized in the same manner by the reactions of starting chlorides and large excess of anhydrous hydrogen fluoride (aHF), and vacuum-stable liquid salts of various cations, such as alkylimidazolium and alkylpyrrolidinium, possess the same HF composition formulated by $[cation]^+(FH)_{2.3}F^-$ at room temperature [15-18]. They are composed of a cation and two kinds of fluorohydrogenate anions, $(FH)_2F^-$ and $(FH)_3F^-$, as shown in Fig. 2, in the ratio required to yield the composition shown above.

The reactions of amines and esters directly yielding alkylammonium salt are also used for the preparation of ILs. For example, the reaction of 1-ethylimidazole and methyltriflate ($MeOSO_2CF_3$) in 1,1,1-trichloroethane yields $[EMIm]CF_3SO_3$ [10]. This reaction does not produce any byproducts and is regarded as a clean method, although a rigorous anhydrous condition is required to avoid hydrolysis.

$$\text{1-ethylimidazole} + CH_3OSO_2CF_3 \rightarrow [EMIm]CF_3SO_3 \quad (4)$$

Salts of tertiary ammonium cations are prepared by the neutralization of the starting tertiary amine with acid. For example, 1-methylimidazolium tetrafluoroborate ($[MeIm]BF_4$) is synthesized by the neutralization of 1-methylimidazole by HBF_4 [19].

$$\text{1-methylimidazole} + HBF_4 \rightarrow [MeIm]BF_4 \quad (5)$$

In the case of tertiary ammonium salts, it should be noted that some molecular species on the left side remain in the reaction product due to the equilibrium of reaction (5).

A chloroaluminate salt is synthesized by the reaction of a chloride and aluminum trichloride [20,21];

$$[EMIm]Cl + nAlCl_3 \rightarrow [EMIm](AlCl_3)_nCl \qquad (6)$$

where salts with $n<1$, $n=1$ and $n>1$ are termed basic, neutral, and acidic, respectively. Bromoaluminate salts are also obtained in the same manner using corresponding bromides [22]. Tetraalkylammonium fluorides with linear alkyl chains are isolated and the reactions with fluoroacids yield salts of the fluorocomplex anion [23]. On the other hand, alkylimidazolium and alkylpyridinium fluorides are unstable and have never been isolated as solvent-free solids. A monohydrate salt of 1-butyl-3-methylimidazolium fluroride ([BMIm]F·H_2O) has been recently reported to be a decomposition product of [BMIm]PF_6 [24]. Fluorohydrogenates and the solvated fluorides above are convenient starting reagents in which the fluorobasicity is decreased to stabilize the salts. Reactions of [EMIm]$(FH)_{2.3}F$ and some fluoroacids have been recently reported to produce various ILs [25,26].

$$[EMIm](FH)_nF + MF_m \rightarrow [EMIm]MF_{m+1} + nHF \qquad (7)$$

[EMIm]$(FH)_n$F itself is a stable IL with a low viscosity and high conductivity, as will be described below. In reaction (7), only a volatile byproduct is formed to yield salts with high purities.

3 Properties of ionic liquids

ILs containing EMIm cations exhibit superior physical properties, such as low viscosity and high conductivity, and have been extensively studied and reported so far. Some selected physical properties of EMIm-based ILs are listed in Table 1. Physical properties of ILs of other imidazolium cations are summarized in references [6,7].

3.1 Melting points of ionic liquids

Ionic liquids, with the current definition, are usually in a liquid state below 100°C [27]. A room temperature ionic liquid (RTIL) is in the liquid form below 25°C [3]. Many ionic liquids of pure compounds exhibit melting points, however, some of them exhibit only a glass transition. Solidified glassy ionic liquids sometimes crystallize before melting exhibiting an exothermic peak in the DSC curve. This is called revitrification. Thus, ionic liquids exhibit various thermal behaviors when they are cooled to be solidified and heated to be liquefied, which characterize the nature of these materials.

In general, an increase in the size of ions in ionic liquids decreases the electrostatic interaction between the cation and anion which lowers the melting point of the ionic liquid. For example, if a cation constitutes a series of ionic liquids with various anions, a salt of a large and/or asymmetric anion tends to exhibit a lower melting point. Figure 3 shows the relationship between the size of an inorganic anion with relatively high symmetries and melting points of [EMIm]MF_{m+1} (MF_{m+1}: BF_4^-, PF_6^-, AsF_6^-, SbF_6^-, NbF_6^-, TaF_6^-, WF_7^-) [26], where the radius of the central atom in the fluorocomplex anion is plotted on the horizontal axis [28]. [EMIm]PF_6, [EMIm]AsF_6, and [EMIm]SbF_6 are isostructural with each other. At least for the hexafluorocomplex (MF_6^-) salts, the melting point decreases linearly with an increase in the size of the anion. [EMIm]NbF_6 and [EMIm]TaF_6, whose molar volumes are close to each other (190 and 187 $cm^3\,mol^{-1}$), exhibit very close melting points. For the EMIm salts of non-octahedral anions, the relationship between the melting point and anion size for [EMIm]WF_7 is in accordance with that of the octahedral anions whereas [EMIm]BF_4 exhibits a significantly lower melting point than expected from the anionic volume. The tetrahedral BF_4^- anion is expected to have a different interaction with the cation compared to hexa- or heptafluorocomplex anions. In the series of EMIm ionic liquids, [EMIm]$(FH)_{2.3}F$ exhibits a significantly low melting point compared to other EMIm salts in spite of its small sized anions. In the case of ILs of bulky organic anions like $(CF_3SO_2)_2N^-$, there is no clear relationship between the melting points and sizes of the anions. An asymmetric anion,

$(CF_3CO)(CF_3SO_2)N^-$, also yields salts with low melting points when combined with symmetric cations including nonaromatic cyclic alkylammonium cations, with the salts usually exhibiting high melting points [29,30].

3.2 Conductivity and viscosity

Most of the conductivities of ILs range in the order of 10^0 to 10^1 mS cm^{-1} (for example, 14 mS cm^{-1} for [EMIm]BF_4 and 8.4 mS cm^{-1} for [EMIm]$(CF_3SO_2)_2N$), lower than those of aqueous systems (for example, the conductivity of 30 wt% H_2SO_4 is about 800 mS cm^{-1}). Conductivities of organic electrolyte solutions depend on the solute, solvent, and concentration and usually fall in the range of 10^0 to 10^2 mS cm^{-1}. Therefore, it can be stated that conductivities of ILs are similar to, or a little lower than, those of organic electrolytes. The lower conductivities of these non-aqueous electrolytes are mostly a result of their high viscosities. Exceptionally high conductivities are observed for some dialkylimidazolium fluorohydrogenates (~10^2 mS cm^{-1}). An inversely proportional relationship, known as Walden's rule, exists between molar conductivities and viscosities of imidazolium-based ILs;

$$\lambda\eta = \text{constant} \qquad (8)$$

where λ is the molar conductivity and η is the viscosity. Figure 4 shows a Walden plot where the reciprocal molar conductivities of ILs composed of dialkylimidazolium cations and fluoroanions are plotted as a function of their viscosities (DMIm: 1,3-dimethylimidazoium, PrMIm: 1-methyl-3-propylimidazolium, BMIm: 1-butyl-3-methylimidazolium, PeMIm: 1-pentyl-3-methylimidazolium, HMIm: 1-hexyl-3-methylimidazolium). Since the values in the plot are distributed over two orders of magnitude, both the axes are shown as logarithmic scales, with a linear relationship being observed for the plot [17]. The viscosity is again the most decisive factor for the conductivity of these ionic liquids. It should be noted that the plots of 1-alkyl-3-methylimidazolium fluorohydrogenates ([RMIm]$(FH)_{2.3}F$) also appear on the same line.

As mentioned above, [RMIm](FH)$_{2.3}$F salts possess relatively high conductivities which arise from the low viscosities of these salts. The contribution of proton hopping among the fluorohydrogenate anions is ruled out based on the results of pulsed-gradient spin-echo (PGSE) NMR studies of these ionic liquids where the contribution of each ionic species is separately determined [31].

The temperature dependence of the conductivities and viscosities of [RMIm](FH)$_{2.3}$F are shown in Figs. 5 and 6. The linearity of the Arrhenius plots is rather good for these ILs due to the low viscosity at ambient temperatures. However, in general, the conductivities and viscosities of highly viscous ILs do not obey a simple Arrhenius law, and the plots of the logarithmic values of conductivities and viscosities as a function of the inverse of the absolute temperature curve are convex and concave, respectively, as shown in Figs. 7 and 8. In such a case, the Vogel-Tamman-Fulcher (VTF) equation is usually employed instead to express the temperature dependence [32].

$$\kappa = \kappa_0 T^{-1/2} \exp[-B/(T-T_0)] \quad (9)$$

$$\eta = \eta_0 T^{-1/2} \exp[-B/(T-T_0)] \quad (10)$$

where κ and η are the conductivity and viscosity, respectively. B and T_0 are empirically determined constants, the latter termed the ideal glass transition temperature.

3.3 Electrochemical window

A wide electrochemical window is one of the most important factors required for applications of ILs as electrolytes in electrochemical devices with high power and energy. For aqueous solutions, the theoretical electrochemical window is 1.23 V at the standard state. No drastic extension is expected although overvoltages are more or less observed in practice depending on the electrolyte and electrode materials. On the other hand, organic solvents such as propylene carbonate and acetonitrile possess high electrochemical stabilities, leading to electrochemical

windows of more than 4 V. The electrochemical window of ILs is usually measured by cyclic voltammetry using platinum or glassy carbon electrodes as in the case of organic electrolytes. Figure 9 shows cyclic voltammograms of platinum or glassy carbon electrodes in various ILs, where $EMPyr^+$ denotes the *N*-ethyl-*N*-methylpyrrolidinium cation. Nonaromatic cations such as aliphatic or nonaromatic heterocyclic ammonium cations are electrochemically more stable than aromatic cations. Fluoroanions such as $(CF_3SO_2)_2N^-$ or BF_4^-, known as counter anions of supporting electrolytes in lithium batteries and electrical double layer capacitors (EDLC), are also employed as anions of ILs with high electrochemical stability. For instance, the electrochemical window of *N*-butyl-*N*-methylpyrrolidinium bis(trifluoromethylsulfonyl)amide ([BMPyr]$(CF_3SO_2)_2N$) is reported to be about 6 V [33], whereas the electrochemical windows of [EMIm]BF_4 and [EMIm]$(CF_3SO_2)_2N$ are about 4.5 V [10,26]. For fluorohydrogenate salts, the cathodic limits are restricted by H_2 evolution from the $(FH)_nF^-$ anion and reduction of the cation. The reaction occurring at the anodic limits is probably fluorination of the cations with the electrochemical window being about 3.2 V. The use of more stable alkylpyrrolidinium cations extends the anodic limit yielding electrochemical windows of approximately 5 V [18].

4 Applications of ionic liquids in electrochemical devices

Applications of ILs in electrochemical devices is of course as electrolytes. If the ILs possess high ionic conductivities and wide electrochemical windows sufficient for the performance required, they possess considerable potential to be substituted for conventional aqueous and organic electrolytes used in electrochemical devices such as batteries, fuel cells, dye-sensitized solar cells, capacitors, and actuators, owing to their non-flammability and non-volatility. These properties of ILs will significantly improve the safety and durability of the electrochemical devices.

4.1 Electric double layer capacitors (EDLC)

The basic energy-storage mechanism of EDLC is not Faradaic but adsorption-desorption of

ions on electrodes made of materials with large surface areas such as activated carbon. A fast charge-discharge process yields a high power density. For an electrolyte of EDLC, a high conductivity and a wide electrochemical window are required to realize high power and energy densities. Several application of ILs to EDLCs have been reported thus far including [EMIm]$(FH)_{2.3}F$ [34], [EMIm]BF_4 [34-36], [EMIm]NbF_6 [35], [EMIm]TaF_6 [35], [EMIm]CF_3SO_3 [36,37], [EMIm]$(CF_3SO_2)_2N$ [36,37], [EMIm]$(CF_3SO_2)_3C$ [36], [BMIm]BF_4 [37], [BMIm]PF_6 [37], and [BMPyr]$(CF_3SO_2)_2N$ [37]. Nanjundiah *et al.* reported capacitances of various ILs on different electrodes [36]. Roughly, there is tendency for the capacitance in the sequence, aqueous solutions > ILs > organic solutions. Another important observation is that the values of capacitance ($\mu F\ cm^{-2}$) on Hg, glassy carbon, and activated carbon are essentially the same, if the scan rate is sufficiently slow. Lewandowski et al. prepared and tested a series of electrochemical capacitors based on activated carbon powders and ILs as electrolytes[37]. The capacitance values obtained for [EMIm]BF_4, [BMIm]BF_4, [BMIm]PF_6, [EMIm]$(CF_3SO_2)_2N$, and [BMPyr]$(CF_3SO_2)_2N$ are not significantly different (5.2~6.3 $\mu F\ cm^{-2}$ when activated carbon with a surface area of 870 $m^2\ g^{-1}$ was used). They pointed out the existence of Faradaic processes such as redox reactions involving surface functional groups on the activated carbon or electrolyte impurities.

Application as the EDLC eletrolyte of [DEME]$(CF_3SO_2)_2N$ (DEME = *N*,*N*-diethyl-*N*-methyl(2-methoxyethyl)ammonium) was carried out using KOH-activated mesophase pitch-based carbon fibers as the electrode material [38]. In this report, they mixed IL with propylene carbonate (PC) to reduce the viscosity of the electrolyte, since the high viscosity of IL was the major drawback to practical applications. This combination provided a specific capacitance of 56 $F\ g^{-1}$ at 1 $mA\ cm^{-2}$ discharge current density and 3.5 V charging voltage (as shown in Fig. 10), which is better than corresponding values for typical electrolyte systems ([TEA]BF_4/PC, 42 $F\ g^{-1}$ at 1 $mA\ cm^{-2}$, 3.5 V).

[EMIm]CF_3SO_3 could serve both as a source of ions as well as a polymer plasticizer [39]. A polymer electrolyte, PAN/[EMIm]CF_3SO_3/TMS, showed a conductivity of 16 $mS\ cm^{-1}$ and specific capacity of 230 $F\ g^{-1}$, expressed versus the mass of the carbon material when activated

carbon with a surface area of 2600 m^2 g^{-1} was used. High conductivity, wide electrochemical stability range, non-volatility, high energy density (~38 kJ kg^{-1}) and power density (~80 kW kg^{-1}) of the capacitors were reported for this polymer electrolyte.

[EMIm]$(FH)_{2.3}F$ with a high conductivity was also applied to EDLC [34]. Table 2 shows a comparison of some physical properties of electrolytes used for EDLC. Capacitance and resistance were measured using coin type cells with activated carbon electrodes (coconuts shell charcoal). [EMIm]$(FH)_{2.3}F$ possesses much lower resistance and larger capacitance than [EMIm]BF_4. However, the electrochemical window for [EMIm]$(FH)_{2.3}F$ is about 3 V and smaller than those of other ILs. In practical EDLC, the cell voltage at which the charge-discharge process is stably performed is about 2 V, which causes a lowering of the energy density. The application of alkylpyrrolidinium and alkylpiperidnium fluorohydrogenates, which have larger electrochemical windows, as EDLC electrolytes is now under investigation.

4.2 Fuel cells

In the case of polymer electrolyte membrane fuel cells (PEMFC) using perfluoroalkylsulfonate membranes such as Nafion®, protons produced at the anode migrate in the electrolyte to react with oxygen forming water at the cathode. This process requires humidification of the electrolyte membrane to maintain its ionic conduction**,** limiting the operational temperature of the system to below 80˚C. The operation of PEMFCs at elevated temperatures, 100 ~ 200˚C, enables the reduction in size of the cooling system and improved polarization behavior leading to a reduction in the use of costly precious metal catalysts. ILs are attractive candidates to realize operation of PEMFCs at elevated temperatures. Some protic acids also have been applied for this purpose. Susan et al. have reported the combination of various organic amines and $HN(SO_2CF_3)_2$ [40]. Although not many of the equimolar conditions of the amine and $HN(SO_2CF_3)_2$ exhibit the liquid state at room temperature, most of them melt below 130˚C and their conductivities are on the order of 10^1 mS cm^{-1} at 130˚C. Details on the fuel cell operation using imidazole with the same concept have been reported separately [41]. The equimolar compound [ImH]$(CF_3SO_2)_2N$ ([ImH]:

imidazolium) exhibits a high melting point of 73˚C. The mixtures exhibit lower melting points than room temperature in both the imidazole- and $HN(SO_2CF_3)_2$-rich composition ranges. Interestingly, imidazole-rich compositions exhibit higher conductivities. These high conductivities can be explained by the proton hopping conduction mechanism among the imidazole molecules. These systems are electrochemically active for H_2 oxidation and O_2 reduction at a Pt electrode under non-humidifying conditions.

Proton-conducting gelatinous electrolytes, templated by $[BMIm]BF_4$ in methylsisesquioxane-backbone-containing H_3PO_4, are thermally and mechanically stable up to 300^{o}C [42]. The electrolyte RTIL/Si/H_3PO_4 with a molar ratio of 0.3/1/1 shows proton conductivity of 1.2 mS cm^{-1} at room temperature, and its electrochemical window is up to 1.5 V. Navarra and coworkers also prepared gel-type membranes using $[DMPIm](CF_3SO_2)_2N$ (DMPIm = 1,2-dimethyl-3-propylimidazolium) as the plasticizer for a poly(vinylidene)fluoride (PVdF) polymer matrix and CF_3SO_3H as the strong organic acid [43]. They reported that the conductivities of the membranes were stable, with values of ca. 2 mS cm^{-1} at room temperature. The conductivities of the membranes increased with increasing temperature, up to 10 mS cm^{-1} at 100^{o}C.

The use of Brønsted acidic ionic liquids to attach to a polyamidoamide dendrimer stable up to 250^{o}C was attempted. The conductivity of the resulting ionic liquid-based membrane was 2.21 mS cm^{-1} at 24^{o}C, suggesting that this ionic liquid can be used as a proton conductor for fuel cell electrolytes over a wide temperature range [44].

Ohno and his coworkers also reported binary ionic liquids, consisting of a zwitterionic liquid and $(CF_3SO_2)_2NH$, for anhydrous proton transport [45]. The conductivity of the Bim3S (1-(1-butyl-3-imidazolio)propane-3-sulfonate) and $(CF_3SO_2)_2NH$ mixture is ca. 0.1 mS cm^{-1} at room temperature, and increases with increasing temperature to 10 mS cm^{-1} at 150^{o}C (Fig. 11).

Fluorohydrogenate anions, $(FH)_nF^-$, do not respond to H_2 and O_2 gases, thereby exhibiting stable electrode potential. Using $[EMIm](FH)_{2.3}F$ as an electrolyte, a new fuel cell concept has been proposed wherein hydrogen is transferred via fluorohydrogenate conduction (Fig. 12) [46].

The cell exhibits an open circuit voltage of more than 1 V between H_2 and O_2 gas electrodes in [EMIm](FH)$_{2.3}$F at 25˚C. Polarization behavior of H_2 and O_2 electrodes in [EMIm](FH)$_{2.3}$F at 25˚C are shown in Fig. 13. A significantly small overpotential of the H_2 electrode in [EMIm](FH)$_{2.3}$F is found compared to that in 30 wt% KOH aqueous solution, whereas the overpotential of O_2 gas electrodes are comparable with each other. Since [EMIm](FH)$_{2.3}$F has HF dissociation pressure at higher temperatures, [EMIm](FH)$_{1.3}$F obtained by eliminating HF under vacuum at 100˚C is used as an electrolyte for operation at 100˚C. Open circuit voltages of the cell using [EMIm](FH)$_{1.3}$F as the electrolyte at 25˚C and 100˚C are again more than 1 V. For comparison with [EMIm](FH)$_{2.3}$F, the polarization behavior of H_2 and O_2 electrodes in [EMIm](FH)$_{1.3}$F at 25˚C and 100˚C are also shown in Fig. 13. Since rearrangement of $(FH)_nF^-$ bonds is involved in the electrode reactions, overpotentials of both the electrodes in [EMIm](FH)$_{1.3}$F are higher than those in [EMIm](FH)$_{2.3}$F due to the stronger $(FH)_n$–F bonds in [EMIm](FH)$_{1.3}$F. However, polarization behavior of both the electrodes is significantly improved at 100˚C compared to 25˚C.

4.3 Lithium batteries

The application of ILs to lithium batteries started in the early stages of research on ILs [47]. The main purpose was to use them as substitutes for organic solvents and to improve battery safety, taking advantage of the non-flammable characteristics of ILs. The ILs of BF_4^- and $(CF_3SO_2)_2N^-$ combined with lithium salts of the same anions have been mostly studied, as shown in Table 3 [48,49]. Applications of EMIm-based ILs as electrolytes of lithium secondary batteries have been reported by several authors, however, the reduction potential is too high for this purpose. Lithium secondary batteries cell performance using EMIm, TMPA (trimethylpropylammonium), PMPyr, and PMPip salts combined with $(CF_3SO_2)_2N^-$ were examined using two-electrode cells. A comparison of the electrochemical windows is shown in Fig. 14 [30]. Here, Li$(CF_3SO_2)_2$N was dissolved in the ILs as a supporting electrolyte, and Li metal and $LiCoO_2$ were used as the negative and positive electrode materials, respectively. Cell tests using [PMPip]$(CF_3SO_2)_2$N

exhibited the best performance among these, which is due to the high stability of the PMPip cation against reduction.

There are three primary ways to use ILs avoiding cathodic reduction. One is to use more stable cations such as 2-substituted imidazolium [50], tetraalky ammonium [51,52], pyrrolidinium [33], and piperidinium [30] cations. ILs consisting of such cations have been found to exhibit better cathodic stability and/or stability toward lithium; however, they still suffer from low ionic conductivity. Another is the use of additives, forming a solid electrolyte interface (SEI) film on the negative electrode, which kinetically prevents cathodic reduction. Additives like HCl [53], $SOCl_2$ [54-56], and H_2O [57] have been reported to be effective for forming a protective film on the lithium surface. Organic solvents, commonly used as lithium battery electrolytes, are also effective to improve lithium deposition/dissolution behavior [58]. However, protic solvents may inhibit cell reactions occurred at both cathode and anode. Aprotic solvents may not have such an inhibitory effect, but they could possible diminish the advantages of using ionic liquid-based electrolytes. The alternative solution is to employ other cathodes possessing a higher reduction potential instead of lithium or LiC_6. Some lithiated metal oxides are used for this purpose and one example is described below. Another important problem to solve is the reduction of the inner resistance of the cell. Non-aromatic cation-based salts are usually highly viscous to have low conductivities. Moreover, addition of the lithium supporting electrolyte also increases the viscosity of the electrolyte.

In the presence of $SOCl_2$ in the chloroaluminate-containing IL, the charge-discharge properties of the graphitized carbon electrode become improved. A discharge capacity of 300 mAh g^{-1} has been demonstrated as long as the electrode is fabricated without a binder. The coulombic efficiency of each cycle is reported to be more than 90% except for the first cycle of nearly 40%. The irreversible capacity observed in the initial charge is thought to be used for the cathodic decomposition of $SOCl_2$ and lead to the SEI formation [56].

Fung and his coworker investigated the applicability of the [EMIm]Cl/$AlCl_3$·$LiAlCl_4$ room temperature ionic liquid system for lithium ion battery [55]. They show that the stability of the

neutral ionic liquid and the reversibility of the lithium electrode in the melt are improved by the addition of $C_6H_5SO_2Cl$, which can be attributed to the removal of $Al_2Cl_7^-$ in the melt. A cycling test with LiAl/$Li_{1-x}CoO_2$ battery using RTIL as the electrolyte showed an average cell voltage of 3.45 V with over 90% coulombic efficiency and a discharge capacity of 112 mAh g^{-1} at current density of 1 mA cm^{-2}.

Sakaebe and his coworker demonstrated that quaternary ammonium-based RTILs are highly stable against the reduction on the lithium metal [30]. They showed that the high coulombic efficiency close to 100% could be achieved with six-membered ring compound [PP13]$(CF_3SO_2)_2N$ (PP13: *N*-methyl-*N*-propylpyridinium). The discharge capacity decreased with the cycle proceeded and became stable to be 87 mAh g^{-1} around 50th cycle.

Nakagawa has reported physical properties of the salt mixtures of $[EMIm]BF_4$ and $LiBF_4$ [48,59]. The conductivity of the system decreases with an increase in the $LiBF_4$ content. $[EMIm]BF_4$ containing 0.15 mol dm^{-3} of $LiBF_4$ exhibits a conductivity of more than 10^0 mS cm^{-1} which is still applicable for a lithium battery. The melting point of the system also decreases with an increase in the amount of $LiBF_4$ in the mixture. Thermal decomposition of $[EMIm]BF_4$ – $LiBF_4$ mixtures occurs at much higher temperatures than that of ethylenecarbonate (EC)/γ-butyloractone (GBR). EC/GBR containing 1 mol dm^{-3} $LiBF_4$ releases organic solvents at 100°C and decomposes at around 200°C, whereas $[EMIm]BF_4$ containing 1 mol dm^{-3} $LiBF_4$ is stable even at 300°C. A cell test of $[EMIm]BF_4$/$LiBF_4$ electrolyte was performed [48] using $Li_4Ti_5O_{12}$ as an anode electrode material. Since the intercalation/deintercalation potential of $Li_4Ti_5O_{12}$ is around 1.5 V vs. Li^+/Li, even EMIm cation-based salts, which are weak against reduction, can be used as electrolytes. The open circuit voltage of the cell at the end of a 1 h rest time before the third discharge with a current of 25 μA cm^{-2} was 2.61 V. This cell showed good performance when it was subjected by low rate charge and discharge.

The lithium cation, which is small in size, is a strong Lewis acid and interacts strongly with the counter anion of the salt, resulting in its high melting point and viscosity. Fujinami and Buzoujima reported room temperature molten lithium salts combined with large anions with an

aluminum center bound to four oxygen atoms (Fig. 15) [8]. Two of the oxygen atoms are bound to fluoroalkyl groups and the others are bound to long ether chains. This weakly coordinating anion functions well to lower the melting point and promotes the dissociation of the cation and anion. Unfortunately, the viscosity of this Li-based IL is still very high which needs to be overcome as the next step for practical applications.

Shin and his coworkers investigated the effect of RTILs on the conductivity of polymer electrolytes [60]. The electrolyte consisting of $P(EO)_{20}(CF_3SO_2)_2NLi$ and $[PYR_{13}](CF_3SO_2)_2N$ (PYR_{13} = *N*-methyl-*N*-propylpyrrolidinium) electrolyte has a lithium ion conductivity of ~ 0.1 mS cm^{-1} at 20°C, whereas the IL-free $P(EO)_{20}(CF_3SO_2)_2NLi$ electrolyte exhibits a Li ion conductivity of only 2×10^{-3} mS cm^{-1}, clearly demonstrating that the conductivity of polymer electrolytes is significantly improved by the incorporation of IL. This system exhibits a stable cycling behavior for about 500 cycles with only a moderate capacity decrease (<0.06% $cycle^{-1}$) at a rate of 0.05 C at 40°C, and no dendritic growth of lithium was observed [61]. The addition of IL to the polymer electrolyte also increases the cell capacity up to 3~4 times even though the value is still not sufficiently high for practical purposes.

Garcia and his coworkers reported that the battery containing $[EMIm](CF_3SO_2)_2N$ and $(CF_3SO_2)_2NLi$ showed better cycling stability compared to those containing $LiBF_4$/$[EMIm]BF_4$ or $(CF_3SO_2)_2NLi$/EC/DMC [62].

Egashira and his coworkers showed that the cycle performance of non-cyclic quaternary ammonium-based ionic liquids could be improved by the introduction of a cyano group onto the ionic liquids. This result indicates that ionic liquids with sufficient conductivity and cycle stability in the lithium deposition/dissolution process can be designed by introducing appropriate functional groups [63].

4.4 Solar cells

ILs are non-volatile which is an important characteristic for the application in solar cells. Grätzel's group originally invented $(CF_3SO_2)_2N$ –based salts to prevent the loss of the electrolyte

solvent by vaporization in dye-sensitized solar cells that they developed [64]. Monohalide IL, 1-hexyl-3-methylimidazolium iodide ([HMIm]I) forms a I^-/I_3^- redox couple when mixed with I_2. The output power of a solar cell is approximately proportional to the product of its electromotive force and maximum current output. The electromotive force is governed by the energy levels of the materials and the current depends on the diffusion rate of the redox species when electron conduction in the semiconductor is sufficiently fast. Therefore, ILs with low viscosities are preferable to facilitate the diffusion of the redox species. Dye-sensitized solar cells based on a ruthenium dye and ionic liquid yield an unprecedented overall conversion efficiency of 9%. Solar cells employing the ruthenium dye with amphiphilic chains in combination with a binary ionic liquid electrolyte yield an efficiency of over 7% while maintaining stability under light absorption at 60°C for 1000 h [65].

The cell performance of solar cells was compared using $[EMIm](FH)_{2.3}F$ and $[EMIm](CF_3SO_2)_2N$ as the electrolytes [66]. [DMHIm]I (1,2-dimethyl-3-hexylimidazolium iodide) and I_2 were used as the source of the I^-/I_3^- redox couple. From the I-V characteristics under illumination, shown in Fig. 16, the maximum current density observed for $[EMIm](FH)_{2.3}F$ is about six times larger than that of $[EMIm](CF_3SO_2)_2N$. This is due to the difference in the diffusion rates of I_3^- caused by the difference of the viscosity in the two ILs (5 cP and 28 cP, respectively). The diffusion coefficient of I_3^- in $[EMIm](FH)_{2.3}F$ calculated from the current density of the reduction peak in the cyclic voltammogram using a Pt electrode is 4.3×10^{-6} cm^2 s^{-1}, whereas that in $[EMIm](CF_3SO_2)_2N$ is 7.6×10^{-7} cm^2 s^{-1}.

4.5 Actuators

Actuators are generally structured as a three-layered configuration where the solid polymer electrolyte layer is sandwiched between two conducting polymer layers such as polyaniline (PANI), polypyrrole (PPy), and polythiophene (PT), which can show dimensional changes by ion expulsion/inclusion movement during oxidation or reduction processes. The relative differential expansion between conducting polymer layers results in bending. However, the low ionic

conductivity of the solid polymer electrolyte leads to an intrinsically slow response system. When the solid polymer electrolyte is swollen with an electrolyte solution, the ionic conductivity can be increased but the performance of this system deteriorates by the evaporation of the solvent.

In order to solve this problem, room temperature ionic liquids have been used in an attempt to fabricate electromechanical actuators for their excellent physical and electrochemical properties such as non-volatility and high ionic conductivity. Osteryoung and his coworkers prepared PANI in [EMIm]Cl/$AlCl_3$ and studied its electrochemistry [67,68]. Unfortunately, it was difficult to use this electrolyte composite for practical applications due to the high moisture sensitivity of the chloroaluminate anion.

Polymer-in-ionic liquid electrolytes (PILEs) were prepared by using PANI and PPy both with [BMIm]PF_6 and [EMIm]$(CF_3SO_2)_2N$ (Fig. 17) [69-71]. Cyclic voltammetric studies of PPy/PF_6/Pt/PVDF/PILE electrochemical actuators showed that the PPy was stable, and a strain of ±2% was observed when a potential of ±2.0 V was applied. This system was subjected to continuous pulsing for more than 3,600 cycles without degradation [70,71]. Mattes and Lu also observed good electroactivity and actuation in the [BMIm]BF_4 electrolyte by doping the PANI with CF_3SO_3H, suggesting a strong interaction between the $CF_3SO_3^-$ dopant of the polymer and the BMIm cation. This actuator showed an excellent lifetime of over 100,000 redox cycles at high potential pulsing (±2.5 V, 0.5 sec) [72].

Another important drawback of present actuator systems is delamination, which limits the actuator life; this is due to poor cohesion between the conducting polymer, the metal layer, and the flexible solid polymer electrolyte. To overcome this problem, Chevrot and coworkers introduced a semi-interpenetrating polymer network (sIPN) wherein poly(3,4-ethylenedioxithiophene) (PEDOT) as a conducting polymer was embedded in an elastomeric polybutadiene/poly(ethylene oxide) IPN matrix with [EMIm]$(CF_3SO_2)_2N$ [73]. This actuator film was subjected to a test of 7×10^6 cycles (f = 10 Hz) for one month without showing degradation and/or delamination. Polymer supported gelatinous RTIL containing single-walled carbon nanotubes, termed bucky-gel, was also adopted for this purpose [74]. When an electric

potential of ±3.0 V was applied with a frequency of 0.1 Hz, an actuator strip underwent a bending motion toward the anode side with a maximum displacement of 1.8 mm (Fig. 18). The actuation was repeated over 8,000 cycles, only with a 20% initial decrease in the actuator stroke in the case of [BIMm]BF_4 when ±2.0 V square-wave input signals were applied at a frequency of 0.1 Hz.

5. Concluding Remarks

Ionic liquids have been interested in various research and industrial fields for their unique properties; non-volatility, non-flammability, wide thermal and electrochemical windows of stability, high ionic conductivity, and wide liquid temperature ranges. It has been demonstrated that ILs suitable for each purpose can be prepared by the proper combination of various cations and anions. The studies for applications of ILs are now in their early stages, however, it shows remarkable progress, especially in the fields of electrochemistry such as capacitors, fuel cells, lithium batteries, solar cells, and actuators for their excellent thermal and electrochemical properties.

Figure captions

Fig. 1 Cations used for the syntheses of ILs.

Fig. 2 Fluorohydrogenate anions: (a) μ-fluoro-bis(fluorohydrogenate) ion ($(FH)_2F^-$), (b) μ_3-fluoro-tris(fluorohydrogenate) ion ($(FH)_3F^-$).

Fig. 3 Relationship between the anion size and the melting point for $[EMIm]MF_{m+1}$. The horizontal axis is referenced to the value of the radius of the central atom of the anion reported by R. D. Shannon, and the radius of seven-coordinated Mo(VI) is used for that of WF_7^- [26-28].

Fig. 4 Walden plot of ionic liquids composed of alkylimidazolium cation and fluoroanions including the present salts. (1) $[EMIm](FH)_{2.3}F$, (2) $[DMIm](FH)_{2.3}F$, (3) $[PrMIm](FH)_{2.3}F$, (4) $[BMIm](FH)_{2.3}F$, (5) $[PeMIm](FH)_{2.3}F$, (6) $[HMIm](FH)_{2.3}F$, (7) 1,3-diethylimidazolium bis(trifluoromethylsulfonyl)amide, (8) $[EMIm]BF_4$, (9) $[DMIm](CF_3SO_2)_2N$, (10) 1-ethyl-3,4-dimethylimidazolium bis(trifluoromethylsulfonyl)amide, (11) 1,3-dimethyl-4-methylimidazolium bis(trifluoromethylsulfonyl)amide, (12) $[EMIm]CF_3CO_2$, (13) 1,3-diethylimidazolium triflate, (14) 1,3-diethylimidazolium trifluoromethylcarboxylate, (15) 1-ethyl-3,4-dimethylimidazolium triflate, (16) $[BMIm](CF_3SO_2)_2N$, (17) 1-etoxymethyl-3-methylimidazolium bis(trifluoromethylsulfonyl)amide, (18) 1-ethyl-2,3-dimethylimidazolium bis(trifluoromethylsulfonyl)amide, (19) $[BMIm]CF_3SO_3$, (20) 1-isobutyl-3-methylimidazolium bis(trifluoromethylsulfonyl)amide, (21) $[BMIm]CF_3CO_2$, (22) 1-butyl-3-ethylimidazolium trifluoromethylcarboxylate, (23) $[BMIm]CF_2CF_2CF_3CO_2$, (24) 1-(2,2,2-trifluoromethyl)-3-methylimidazolium bis(trifluoromethylsulfonyl)amide, (25) 1-butyl-3-ethylimidazolium perfluorobutylsulfate, (26) $[BMIm]CF_3CF_2CF_2CF_2SO_3$. Viscosities and conductivities of the salts were obtained in the present study or are summarized in references 6 and 7.

Fig. 5 Arrhenius plots of the conductivities of [RMIm]$(FH)_{2.3}F$ [17].

Fig. 6 Arrhenius plots of the viscosities of [RMIm]$(FH)_{2.3}F$ [17].

Fig. 7 Arrhenius plots of the conductivities of selected ILs [10].

Fig. 8 Arrhenius plots of the viscosities of selected ILs [10].

Fig. 9 Electrochemical windows of some ILs measured by cyclic voltammetry. Working electrodes: glassy carbon for [EMPyr]$(FH)_{2.3}F$ and [EMIm]$(FH)_{2.3}F$ and platinum for [EMIm]TaF_6 and [EMIm]BF_4 [17,18,25,26].

Fig. 10 Effect of the charging voltage on the capacitance uptake using [DEME]BF_4 (IL-B), [DEME]$(CF_3SO_2)_2N$ (IL-T), and conventional [TEA]BF_4 in PC with 0.8 and 1 molar fraction. (a, b) The variation of the gravimetric (F/g) capacitance obtained at 1 and 10 mA cm^{-2} discharge current density, respectively [38].

Fig. 11 Temperature dependence of the ionic conductivity for the Bim3S/$(CF_3SO_2)_2NH$ mixture (mole fraction of Bim3S is 60%) [45].

Fig. 12 Principle of the fuel cell of [EMIm]$(FH)_{2.3}F$ [46].

Fig. 13 Polarization behavior of (a) H_2 and (b) O_2 gas electrodes in [EMIm]$(FH)_{2.3}F$, [EMIm]$(FH)_{1.3}F$ and 30 wt% KOH [46].

Fig. 14 Electrochemical windows of some ILs for electrolytes of lithium batteries measured by linear sweep voltammetry. W.E.: glassy carbon, C.E.: Pt, R.E.: Pt [30].

Fig. 15 Structures of room temperature molten lithium salts with large aluminate anions [8].

Fig. 16 I-V characteristics of a cell using [EMIm]$(FH)_{2.3}F$ and [EMIm]$(CF_3SO_2)_2N$ containing 0.9 M of [DMHIm]I and 30 mM of I_2 [66].

Fig. 17 Cross-section of PPy double-sided PVDF electrochemical actuator using a polymer-in-ionic liquid as electrolyte [70].

Fig. 18 Performance of a bucky-gel actuator (15 mm in length, 1 mm in width, 0.28 mm in thickness) in response to alternating square-wave electric potentials. a) Bending motion of the actuator strip at an applied voltage of ±3.5 V with a frequency of 0.01 Hz. b) Input signals (V), currents (I), and displacements (δ) of the actuator strip at an applied voltage of ±3.0 V with a frequency of 0.1 Hz [74].

Table 1 Physical properties of EMIm cation-based ILs

	Melting point / °C	Density at 25 °C / g cm^{-3}	Viscosity at 25 °C / cP	Conductivity at 25 °C / mS cm^{-1}	Ref.
[EMIm]$AlCl_4$	8	1.29	18	22.6	20,21
[EMIm]$(AlCl_3)_2Cl$	-	1.39	14	15.4	20,21
[EMIm]NO_2	55	1.27	-	-	1
[EMIm]NO_3	38	1.28	-	-	1
[EMIm]$(CN)_2N$	-12	1.08	17	27	75
[EMIm]$(CN)_3C$	-11	1.11	18	18	76
[EMIm]FHF	51	1.26			77
[EMIm]$(FH)_{2.3}F$	-65	1.14	5	100	17
[EMIm]BF_4	15	1.28	32	13.6	1,32
[EMIm]PF_6	62	1.56	-	-	78
[EMIm]AsF_6	53	1.78	-	-	26,79
[EMIm]SbF_6	10	1.85	67	6.2	26,80
[EMIm]NbF_6	-1	1.67	49	8.5	25,26
[EMIm]TaF_6	2	2.17	51	7.1	25,26
[EMIm]WF_7	-15	2.27	171	3.2	26
[EMIm]CF_3CO_2	-14	1.29	35	9.6	10
[EMIm]CF_3SO_3	-10	1.38	43	9.3	2,10,36
[EMIm]$(CF_3SO_2)_2N$	-15	1.52	28	8.4	10
[EMIm]$(CF_3CO)(CF_3SO_2)N$	-2	1.46	25	9.8	29
[EMIm]$(CF_3SO_2)_3C$	39	-	181	1.7	10,36

Table 2 Physical properties of electrolytes and cell performance in EDLC cells at 25°C, 0.8 V [34)]

Electrolyte	Conductivity / mS cm^{-1}	Viscosity / cP	Capacitance / F cm^{-3}	Resistance / Ω
$[EMIm](FH)_{2.3}F$	100	4.9	11.1	6.6
$[EMIm]BF_4$	13	43	6.8	19.8
35 wt% H_2SO_4	848	2.5	23.2	4.6
1M $[Et_3MeN]BF_4$/PC	13	3.5	8.1	11.8

Table 3 Lithium batteries using ILs of fluoroanions

Electrolyte	Cathode material	Anode material	Ref.
[EMIm]BF_4 – $LiBF_4$	$LiCoO_2$	$Li_4Ti_5O_{12}$	48,59
[EMIm]BF_4 – $LiBF_4$	$LiCoO_2$	Li-Al	81
[TMPA]$(CF_3SO_2)_2N$ – Li$(CF_3SO_2)_2N$	$LiCoO_2$	Li	30
[PMPip]$(CF_3SO_2)_2N$ – Li$(CF_3SO_2)_2N$	$LiCoO_2$	Li	30
[PMPip]$(CF_3SO_2)_2N$ – Li$(CF_3SO_2)_2N$	Sn	Li	30
[TEA]$(CF_3CO)(CF_3SO_2)N$ – Li$(CF_3SO_2)_2N$	$LiCoO_2$	Li	49
[EMIm]$(CF_3SO_2)_2N$ – Li$(CF_3SO_2)_2N$	$LiCoO_2$	Li	49
[EMIm]$(CF_3CO)(CF_3SO_2)N$ – Li$(CF_3SO_2)_2N$	$LiCoO_2$	Li	49

TMPA: Trimethylpropylammonium, PMPip: *N*-propyl-*N*-methylpiperidinium, TEA: tetraethylammonium,

References

1) J. S. Wilkes, M. J. Zaworotko, J. Chem. Soc., Chem. Commun., 965 (1992).

2) E. I. Cooper, E. J. M. O'Sullivan, Proceedings of 8th International Symposium on Ionic liquids, R. J. Gale, G. Blomgren, and H. Kojima, (Eds.), The Electrochemical Society: Pennington, NJ, 386 (1992).

3) T. Welton, Chem. Rev., **99**, 2071 (1999).

4) K. R. Seddon, J. Chem. Technol. Biotechnol., **68**, 351 (1997).

5) P. Wasserscheid, W. Kein, Angew. Chem. Int. Ed., **39**, 3772 (2000).

6) R. Hagiwara, Y. Ito, J. Fluorine Chem., **105**, 221 (2000).

7) R. Hagiwara, Electrochemistry, **70**, 130 (2002).

8) T. Fujinami, Y. Buzoujima, J. Power Sources, **119-121**, 438 (2003).

9) S. Konno, R. Hagiwara, Abstracts of 73th Annual Meeting of The Electrochemical Society of Japan, 135 (2006).

10) P. Bonhôte, A.-P. Dias, M. Armand, N. Papageorgiou, K. Kalyanasundaram, M. Grätzel, Inorg. Chem., **35**, 1168 (1996).

11) R. P. Singh, S. Manandhar, J. M. Shreeve, Tetrahedron Lett., **43**, 9497 (2002).

12) Z. Zhou, H. Matsumoto, K. Tasumi, Chem. Lett., **33**, 680 (2004).

13) Z. Zhou, H. Matsumoto, K. Tasumi, Chem. Lett., **33**, 886 (2004).

14) D. R. Robin, K. R. Seddon, Ionic Liquids IIIA: Fundamentals, Progress, Challenges, and Opportunities, ACS, Washington, 2005.

15) R. Hagiwara, T. Hirashige, T. Tsuda, Y. Ito, J. Fluorine Chem., **99**, 1 (1999).

16) R. Hagiwara, T. Hirashige, T. Tsuda, Y. Ito, J. Electrochem. Soc., **149**, D1 (2002).

17) R. Hagiwara, K. Matsumoto, Y. Nakamori, T. Tsuda and Y. Ito, H. Matsumoto, K. Momota, J. Electrochem. Soc., **150**, D195 (2003).

18) K. Matsumoto R. Hagiwara, Y. Ito, Electrochem. Solid State Lett., **7**, E41 (2004).

19) M. Hirao, H. Sugimoto, H. Ohno, J. Electrochem. Soc., **147**, 4168 (2000).

20) J. S. Wilkes, J. A. Levisky, R. A. Wilson, C. L. Hussey, Inorg. Chem., **21**, 1263 (1982).

21) A. A. Fanning Jr., D. A. Floreani, L. A. King, S. S. Landers, B. J. Piersma, D. J. Stech, R. L. Vaughn, J. S. Wilkes, J. L. Williams, J. Phys. Chem., **88**, 2614 (1984).

22) J. A. Boon, J. S. Wilkes, J. A. Lanning, J. Electrochem. Soc., **138**, 465 (1991).

23) K. O. Christe, W. W. Wilson, R. D. Wilson, R. Bau, J. A. Feng, J. Am. Chem. Soc. **112**, 7619 (1990).

24) R. P. Swatloski, J. D. Holbrey, R. D. Rogers, Green Chem., **5**, 361 (2003).

25) K. Matsumoto, R. Hagiwara, Y. Ito, J. Fluorine Chem., **115**, 133 (2002).

26) K. Matsumoto, R. Hagiwara, R. Yoshida, Y. Ito, Z. Mazej, P. Benkič, B. Žemva, O. Tamada, H. Yoshino, S. Matsubara, Dalton Trans., 144 (2004).

27) J. S. Wilkes, Green Chemistry, **4**, 73 (2002).

28) R. D. Shannon, Acta Cryst., **A32**, 751 (1976).

29) H. Matsumoto, H. Kageyama, Y. Miyazaki, Chem. Commun. 1726 (2002).

30) H. Sakaebe, H. Matsumoto, Electrochem. Commun. **5**, 594 (2003).

31) Y. Saito, K. Hirai, K. Matsumoto, R. Hagiwara, Y. Ito, Y. Minamizaki, J. Phys. Chem. B, **109**, 2942 (2005).

32) A. Noda, K. Hayamizu, M. Watanabe, J. Phys. Chem. B, **105**, 4603 (2001).

33) D. R. MacFarlane, P. Meakin, J. Sun, N. Amini, M. Forsyth, J. Phys. Chem. B, **103**, 4164 (1999).

34) M. Ue, M. Takeda, A. Toriumi, A. Kominato, R. Hagiwara, Y. Ito, J. Electrochem. Soc., **150**, A499 (2003).

35) M. Ue, M. Takeda, T. Takahashi, M. Takehara, Electrochem. Solid State Lett., **5**, A119 (2002).

36) C. Nanjundiah, S. F. McDevitt, V. R. Koch, J. Electrochem. Soc., **144**, 3392 (1997).

37) A. Lewandowski, M. Galiński, J. Phys. Chem. Solids, **65**, 281 (2004).

38) Y.-J. Kim, Y. Matsuzawa, S. Ozaki, K. C. Park, C. Kim, M. Endo, H. Yoshida, G. Masuda, T. Sato, M. S. Dresselhaus, J. Electrochem. Soc., **152**, A710 (2005).

39) A. Lewandowski, A. Swiderska, Appl. Phys. A, **82**, 579 (2006).

40) M. A. B. H. Susan, A. Noda, S. Mitsushima, M. Watanabe, Chem. Commun., 938 (2003).

41) A. Noda, M. A. B. H. Susan, K. Kudo, S. Mitsushima, K. Hayamizu, M. Watanabe, J. Phys. Chem. B, **107**, 4024 (2003).

42) Z. Li, H. Liu, Y. Liu, P. He, J. Li, J. Phys. Chem. B, **108**, 17512 (2004).

43) M. A. Navarra, S. Panero, B. Scrosati, Electrochem. Soild-State Lett., **8**, A324 (2005).

44) J.-F. Huang, H. Luo, C. Liang, I.-W. Sun, G. A. Baker, S. Dai, J. Am. Chem, Soc., **127**, 12784 (2005).

45) H. Yoshizawa, H. Ohno, Chem. Commun., 1828 (2004).

46) R. Hagiwara, T. Nohira, K. Matsumoto, Y. Tamba, Electrochem. Solid-State Lett., **8**, A231 (2005).

47) J. Devynck, R. Messina, J. Pinggarron, B. Tremillon, L. Trichet, J. Eletctrochem. Soc., **131**, 2274 (1984).

48) H. Nakagawa, S, Izuchi, K. Kuwana, T. Nukuda, Y. Aihara, J. Electrochem. Soc., **150**, A695 (2003).

49) H. Matsumoto, H. Sakaebe, Polymer Preprints, Japan, **51**, 2758 (2002).

50) V. R. Koch, C. Nanjundiah, G. B. Appetecchi, B. Scrosati, J. Electrochem. Soc., **142**, 116 (1995).

51) J. Sun, M. Forsyth, D. R. MacFarlane, J. Phys. Chem. B, **102**, 8858 (1998).

52) M. Matsumoto, M. Yanagida, K. Tanimoto, M. Nomura, Y. Kitagawa, Y. Miyazaki, Chem. Lett., 922 (2000).

53) B. J. Piersma, D. M. Lyan, E. R. Schumacher, T. L. Riechel, J. Electrochem. Soc., **143**,, 908 (1996).

54) J. Fuller, R. A. Osteryoung, R. T. Carlin, J. Electrochem. Soc., **142**, 3632 (1995).

55) Y. S. Fung, R. Q. Zhou, J. Power Sources, **81/82**, 891 (1999).

56) N. Koura, K. Etoh, Y. Idemoto, F. Matsumoto, Chem. Lett., 1320 (2001).

57) J. Fuller, R. T. Carlin, R. A. Osteryoung, J. Electrochem. Soc., **144**, 3881 (1997).

58) M. Egashira, T. Kiyabu, I. Watanabe, S. Okada, J. Yamaki, Electrochemistry, **71**, 1114

(2003).

59) H. Nakagawa, Youyuuenn Oyobi Kouonnkagaku **47**, 19 (2004).

60) J.-H. Shin, W. A. Henderson, S. Passerini, Electrochem. Commun., **5**, 1016 (2003).

61) J.-H. Shin, W. A. Henderson, S. Scaccia, P. P. Prosini, S. Passerini, J. Power Sources, **156**, 560 (2006).

62) B. Garcia, S. Lavallee, G. Perron, C. Michot, M. Armand, Electrochim. Acta, **49**, 4583 (2004).

63) M. Egashira, S. Okada, J. Yamaki, D. A. Dri, F. Bonadies, B. Scrosati, J. Power Sources, **138**, 240 (2004).

64) N. Papageorgiou, Y. Athanassov, M. Armand, P. Bonhôte, H. Pettersson A. Azam, M. Grätzel, J. Electrochem. Soc., **143**, 3099 (1996).

65) D. Kuang, S. Ito, B. Wenger, C. Klein, J.-E Moser, R. Humphry-Baker, S. M. Zakeeruddin, M. Grätzel, J. Am. Chem. Soc., **128**, 4146 (2006).

66) H. Matsumoto, T. Matsuda, T. Tsuda, R. Hagiwara, Y. Ito, Y. Miyazaki, Chem. Lett., 26 (2001).

67) J. Tang. R. A. Osteryoung, Synth. Met., **44**, 307 (1991).

68) J. Tang, R. A. Osteryoung, Synth. Met., **45**, 1 (1991).

69) W. Lu, A. G. Fadeev, B. Qi, E. Smela, B. R. Mattes, J. Ding, G. M. Spinks, J. Mazurkiewicz, D. Zhou, G. G. Wallace, D. R. MacFarlane, S. A. Forsyth, M. Forsyth, Science, **297**, 983 (2002).

70) D. Zhou, G. M. Spinks, G. G. Wallace, C. Tiyapiboonchaiya, D. R. MacFarlane, M. Forsyth, J. Sun, Electrochim. Acta, **48**, 2355 (2003).

71) J. Ding, D. Zhou, G. Spinks, G. Wallace, S. Forsyth, M. Forsyth, D. R. MacFarlane, Chem. Matter., **15**, 2392 (2003).

72) W. Lu, B. R. Mattes, Synth. Met., **152**, 53 (2005).

73) F. Vidal, C. Plesse, D. Teyssié, C. Chevrot, Synth. Met., **142**, 287 (2004).

74) T. Fukushima, K. Asaka, A. Kosaka, T. Aida, Angew. Chem. Int. Ed. **44**, 2410 (2005).

75) D.R. MacFarlane, J. Golding, S. Forsyth, M. Forsyt, G.B. Deacon, Chem. Commun., 1430

(2001).

76) Y. Yoshida, K. Muroi, A. Otsuka, G. Saito, M. Takahashi, T. Yoko, Inorg. Chem., **43**, 1458 (2004).

77) K. Matsumoto, T. Tsuda, R. Hagiwara, Y. Ito, O. Tamada, Solid State Sci., **4**, 23 (2002).

78) J. Fuller, R.T. Carlin, H.C. De Long, D. Haworth, J. Chem. Soc., Chem., Commun., 299 (1994).

79) A. B. McEwen, H. L. Ngo, K. LeCompte, J. L. Goldman, J. Electrochem. Soc., **146**, 1687 (1999).

80) C. H. Song, W. H. Shim, E. J. Roh, J. H. Choi, J. Chem. Soc., Chem. Commun., 1695 (2000).

81) R. T. Carling, J. Fuller, W. K. Kuhn, J. Lysaght, P. C. Trulove, J. Appl. Electrochem., **26**, 1147 (1996).

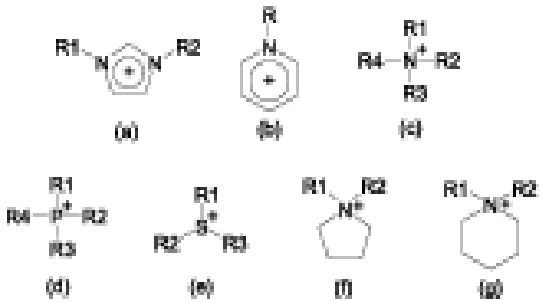

Fig. 1 Cations used for the syntheses of ILs.

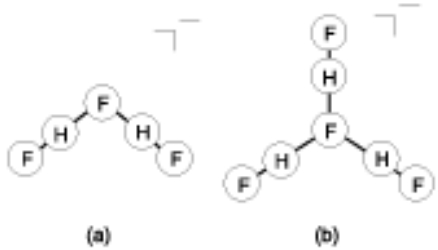

Fig. 2 Fluorohydrogenate anions: (a) μ-fluoro-bis (fluorohydrogenate) ion ($(FH)_2F^-$), (b) μ_3-fluoro-tris (fluorohydrogenate) ion ($(FH)_3F^-$).

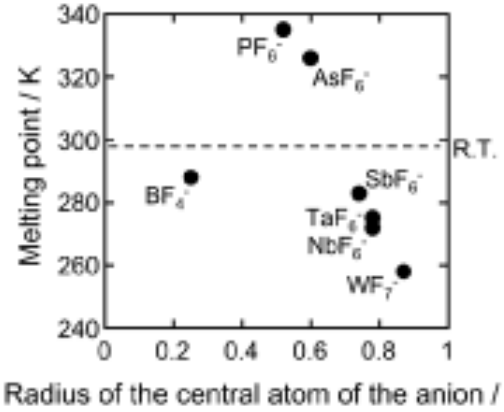

Fig. 3 Relationship between the anion size and the melting point for $[EMIm]MF_{m+1}$. The horizontal axis is referenced to the value of the radius of the central atom of the anion reported by R. D. Shannon, and the radius of seven-coordinated Mo(VI) is used for that of WF_7^-.[28-29]

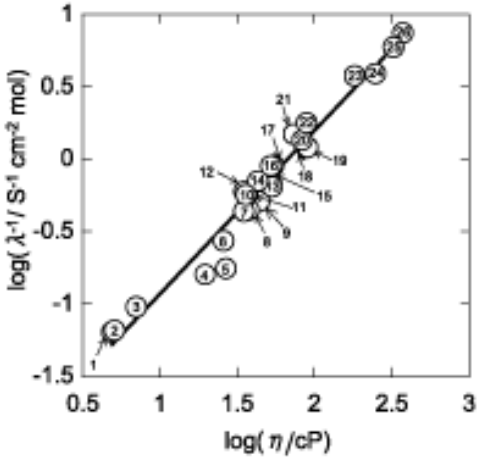

Fig. 4 Walden plot of ionic liquids composed of alkylimidazolium cation and fluoroanions including the present salts. (1) $[EMIm](FH)_{2.3}F$, (2) $[DMIm](FH)_{2.3}F$, (3) $[PrMIm](FH)_{2.3}F$, (4) $[BMIm](FH)_{2.3}F$, (5) $[PeMIm](FH)_{2.3}F$, (6) $[HMIm](FH)_{2.3}F$, (7) 1,3-diethylimidazolium bis (trifluoromethylsulfonyl)amide, (8) $[EMIm]BF_4$, (9) $[DMIm](CF_3SO_2)_2N$, (10) 1-ethyl-3,4-dimethylimidazolium bis (trifluoromethylsulfonyl)amide, (11) 1,3-dimethyl-4-methylimidazolium bis(trifluoromethylsulfonyl)amide, (12) $[EMIm]CF_3CO_2$, (13) 1,3-diethylimidazolium triflate, (14) 1,3-diethylimidazolium trifluoromethylcarboxylate, (15) 1-ethyl-3,4-dimethylimidazolium triflate, (16) $[BMIm](CF_3SO_2)_2N$, (17) 1-etoxymethyl-3-methylimidazolium bis (trifluoromethyl-sulfonyl)amide, (18) 1-ethyl-2,3-dimethylimidazolium bis(trifluoromethylsulfonyl)amide, (19) $[BMIm]CF_3SO_3$, (20) 1-isobutyl-3-methylimidazolium bis(trifluoromethyl-sulfonyl)amide, (21) $[BMIm]CF_3CO_2$, (22) 1-butyl-3-ethylimidazolium trifluoromethylcarboxylate, (23) $[BMIm]CF_2CF_2CF_3CO_2$, (24) 1-(2,2,2-trifluoromethyl)-3-methylimidazolium bis(trifluoromethylsulfonyl)amide, (25) 1-butyl-3-ethylimidazolium perfluorobutylsulfate, (26) $[BMIm]CF_3CF_2CF_2CF_2SO_3$. Viscosities and conductivities of the salts were obtained in the present study or are summarized in references 6 and 7.

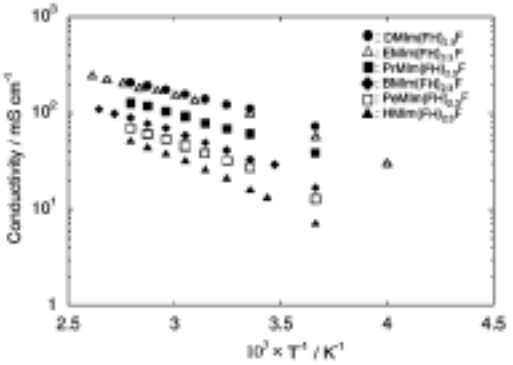

Fig. 5 Arrhenius plots of the conductivities of $[RMIm](FH)_{2.3}F$.[17]

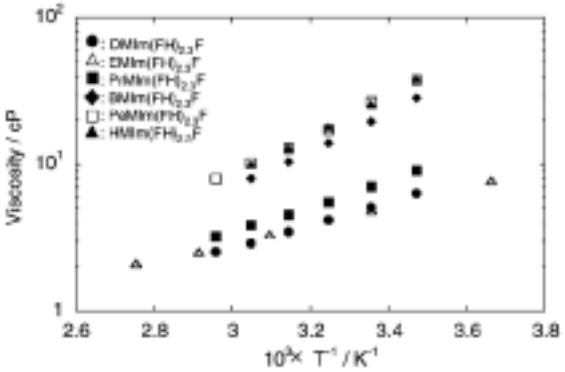

Fig. 6 Andrade plots of the viscosities of $[RMIm](FH)_{2.3}F$.[17]

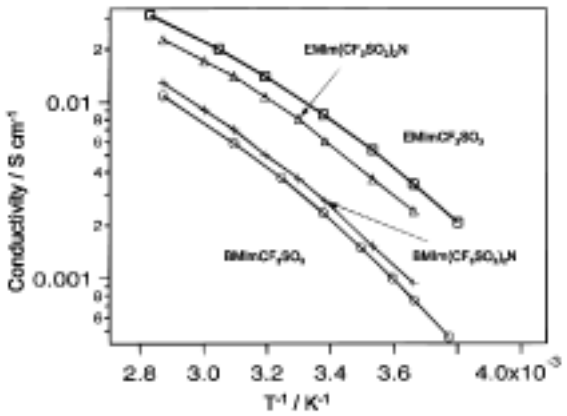

Fig. 7 Arrhenius plots of the conductivities of selected ILs.[10]

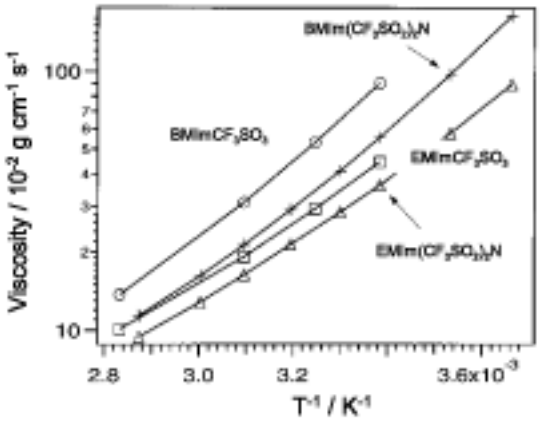

Fig. 8 Andrade plots of the viscosities of selected ILs.[10]

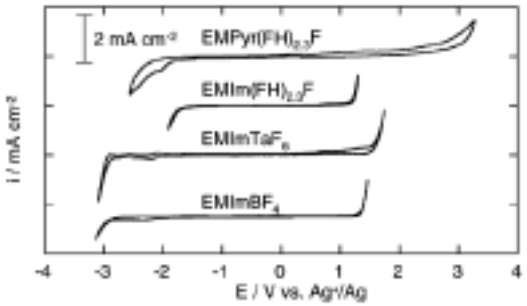

Fig. 9 Electrochemical windows of some ILs measured by cyclic voltammetry. Working electrodes: glassy carbon for [EMPyr](FH)$_{2.3}$F and [EMIm](FH)$_{2.3}$F and platinum for [EMIm]TaF$_6$ and [EMIm]BF$_4$.[17,18,25,26]

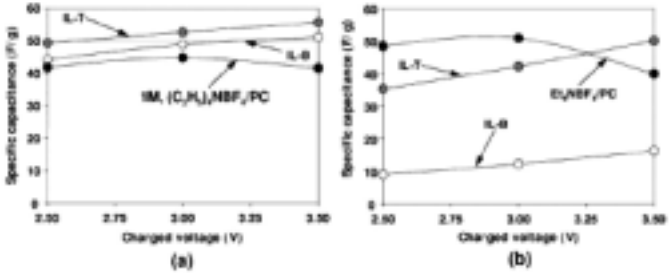

Fig. 10 Effect of the charging voltage on the capacitance uptake using [DEME]BF$_4$ (IL-B), [DEME](CF$_3$SO$_2$)$_2$N (IL-T), and conventional [TEA]BF$_4$ in PC with 0.8 and 1 molar fraction. (a, b) The variation of the gravimetric (F/g) capacitance obtained at 1 and 10 mA cm^{-2} discharge current density, respectively.[28]

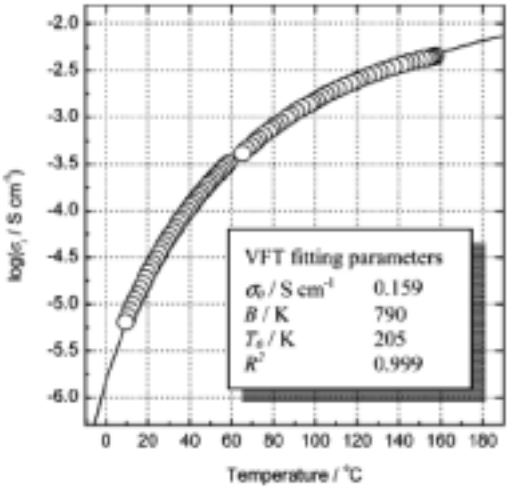

Fig. 11 Temperature dependence of the ionic conductivity for the Bim3S/$(CF_3SO_2)_2NH$ mixture (mole fraction of Bim3S is 60 %).[45]

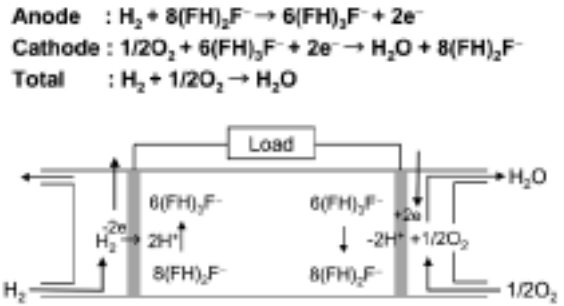

Fig. 12 Principle of the fuel cell of $[EMIm](FH)_{2.3}F$.[40]

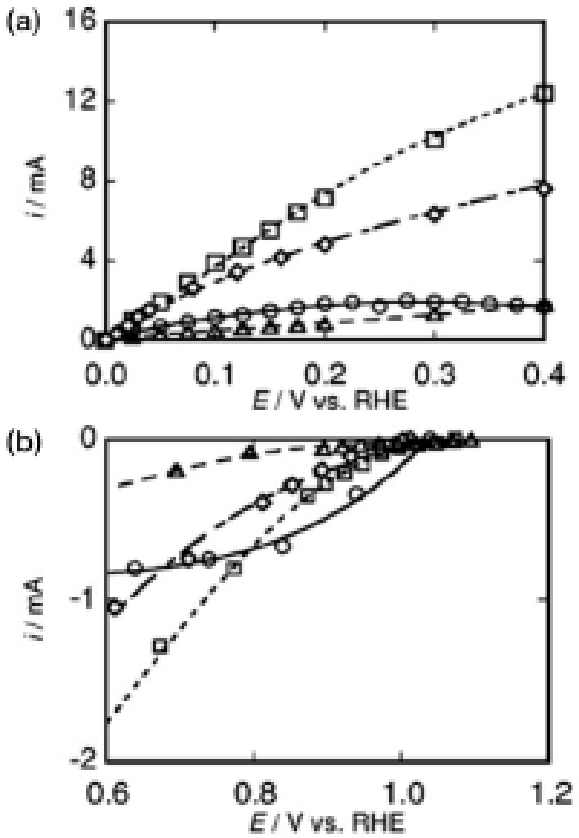

Fig. 13 Polarization behavior of (a) H_2 and (b) O_2 electrodes in $[EMIm](FH)_{2.3}F$ at 25 ℃ (□), $[EMIm](FH)_{3}F$ at 25 ℃ (△), $[EMIm](FH)_{1.2}F$ at 100 ℃ (◇), and 30 wt % KOH solution at 25 ℃ (○).[40]

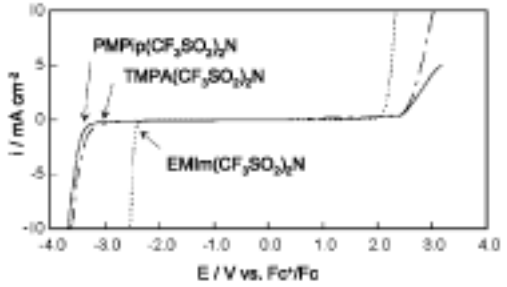

Fig. 14 Electrochemical windows of some ILs for electrolytes of lithium batteries measured by linear sweep voltammetry. W.E.: glassy carbon, C.E.: Pt, R.E.: Pt.[39]

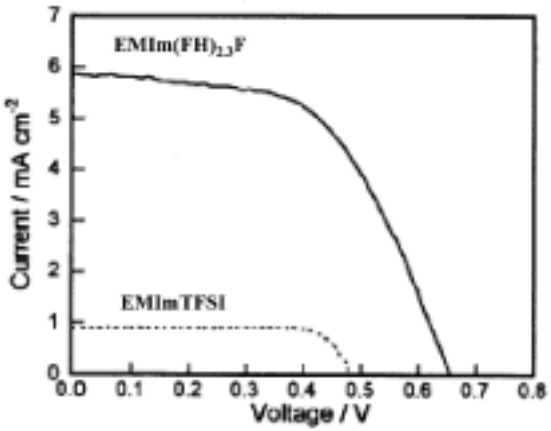

Fig. 16 I-V characteristics of a cell using [EMIm](FH)$_{2.3}$F and [EMIm](CF$_3$SO$_2$)$_2$N containing 0.9 M of [DMHIm]I and 30 mM of I_2.[66]

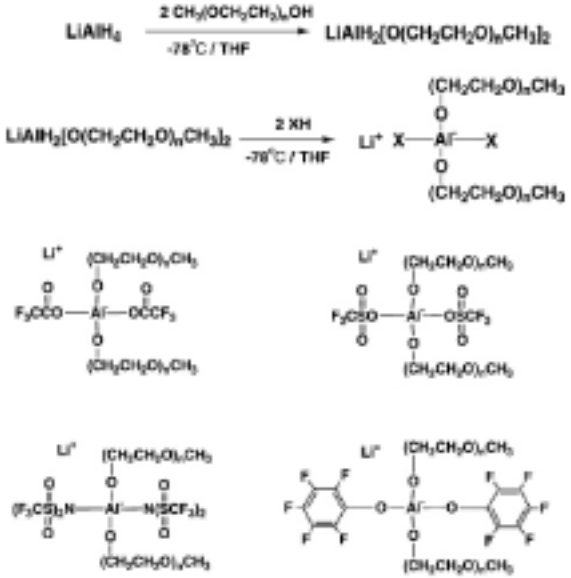

Fig. 15 Structures of room temperature molten lithium salts with large aluminate anions.[8]

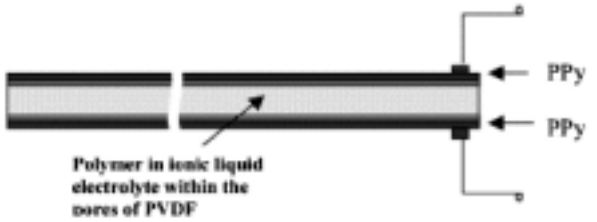

Fig. 17 Cross-section of PPy double-sided PVDF electrochemical actuator using a polymer-in-ionic liquid as electrolyte.[73]

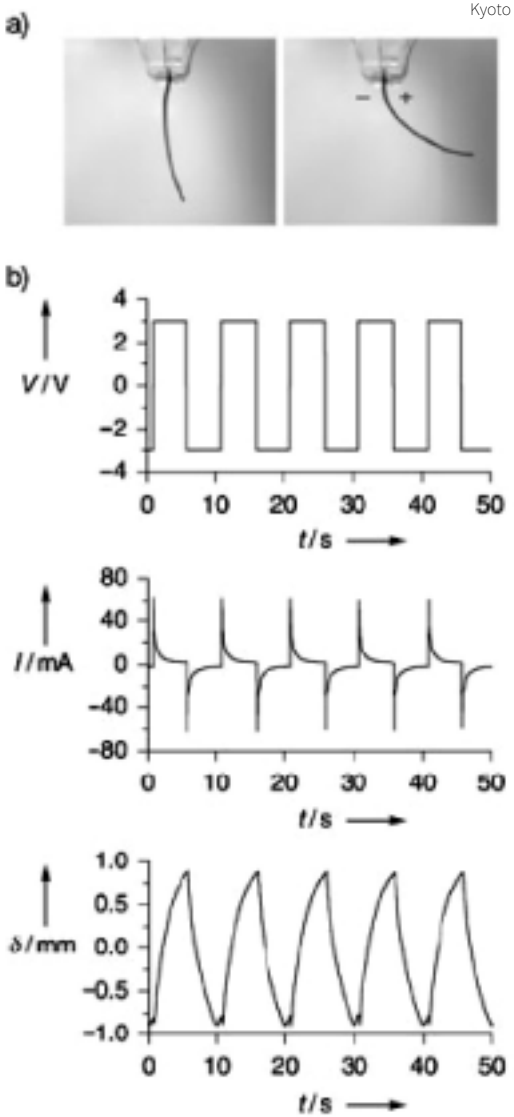

Fig. 18 Performance of a bucky-gel actuator (15 mm in length, 1 mm in width, 0.28 mm in thickness) in response to alternating square-wave electric potentials. a) Bending motion of the actuator strip at an applied voltage of ± 3.5 V with a frequency of 0.01 Hz. b) Input signals (V), currents (I), and displacements (δ) of the actuator strip at an applied voltage of ± 3.0 V with a frequency of 0.1 Hz.[70]